Simulation of Evacuation Processes of Pollutants in the Room Using the Similarity Theory

Marius-Constantin Popescu, Nikos E. Mastorakis, Liliana Popescu

***Abstract*—**Tests on models can provide both information on the verification of calculation methods and solutions that theory currently can not provide. Climate processes occurring in a site are complex and not fully capture the phenomenon of mass transfer of fluid motion and heat. Those basic methods are used hydraulic moulding, which bypass the practical difficulties created by the incompatibility of the conditions of similarity (using areas of forging, hydraulic or geometric distortion).

***Keywords*—**Modelation and Simulation, Polluants and climatisation.

I. INTRODUCTION

IN general, for defining a climatic phenomenon we need two categories of similarity conditions. These conditions are expressed by similar numbers of Reynolds, Froude, Archimedes, etc. the same both real and as model, and resulted from hydraulics equations; solving these equations are experiencing great difficulties, resulting in solutions only for very particular cases. Geometric similarity conditions, the limit and initial (at time t=0) for: speed, temperature, pressure, concentration and mass. To be similar to reality, the model must satisfy all these conditions simultaneously, in different cases remains as a necessary geometric similarity (in which case similar conditions may be reduced in number). To appreciate the necessity of these conditions is useful to know their role. Thus, by Reynolds provided the conditions of geometric similarity ensure cinematic similarity in terms of fixed borders (movement pressure), so reproduction field gear and related phenomena such as energy dissipation, asking the condition Reynolds. These conditions ensure similarity of Froude and Euler dynamic and the correct moulding of pressure field, the forces of connection, conditioned by that cinematic similarity existence. To expand the interpretations and conclusions of several similar phenomena there are used dimensionless coordinates introduced by transformation Ruark [4], [5].

Marius-Constantin Popescu is currently an Associate Professor at the Faculty of Electromechanical and Environmental Engineering, Electromechanical Engineering Department, University of Craiova, ROMANIA, e.mail address popescu.marius.c@gmail.com.

Nikos Mastorakis is currently a Professor in the Technical University of Sofia, BULGARIA, Professor at ASEI (Military Institutes of University Education), Hellenic Naval Academy, GREECE, e.mail address mastor@wseas.org.

Liliana Popescu-Perescu is currently a Teacher in the "E.Cuza" College of Craiova, ROMANIA, e.mail address lpopi2001@yahoo.com

II. THE SIMILARITY BETWEEN REAL AND MODEL CASE

Considering $\vec{i}$ and $\vec{j}$ abscissa unit vectors of the Ox, Oy ordinate respectively, then the movement, speed, time, temperature, pressure (dynamic), viscosity, thermal conductivity and concentration in dimensionless coordinates will be [6], [9]:

$$x_{i*} = \frac{x_i}{A},\ x_{j*} = \frac{x_j}{A},\ v_{i*} = \frac{v_i}{v_0},\ v_{j*} = \frac{vx_i}{v_0},$$

$$t_* = \frac{t}{\frac{A}{v_0}} = \frac{v_I}{A},\ \theta_* = \frac{\theta - \theta_0}{\theta_1 - \theta_0} = \frac{\Delta\theta}{\Delta\theta_0},\ \rho_* = \frac{\rho}{\rho_0 v_0^2},$$

$$\eta_* = \frac{\eta}{\eta_0},\ \lambda_* = \frac{\lambda}{\lambda_0},\ c_* = \frac{c - c_0}{c_1 - c_0},$$

where: A is the height of the layout; x_i, x_j are projections of axes Ox, Oy of movement, v_0 is the velocity of carrier fluid (clean) at the entrance; v_i, v_j are projections of axes Ox, Oy the velocity vector; θ_1 is the fluid temperature;

$\Delta\theta$ temperature is the temperature difference between the pollutant; θ_1 and carrier fluid temperature θ_0 brought in stationary regime; ρ_0 is the mass volume (density) air carrier brought to the entry; η_0 reference is dynamic viscosity; λ thermal conductivity of the fluid carrier is entered; c_1, c_0 pollutant concentrations emitted are respectively the carrier fluid entered.

A.Terms of similarity. Climate phenomena characteristic equations are given in the literature. Thus, the equation of continuity, which expresses the conservation of flow following the direction Ox is

$$\frac{\partial \rho_*}{\partial t_*} + \frac{\partial}{\partial x_{i*}}(\rho_* v_{i*}) = 0\,.$$

Dynamic equation of motion (Navier-Stokes), where the direction Ox is

$$\rho_* \left(\frac{\partial v_{i*}}{\partial t_*} + v_{j*} \frac{\partial v_{i*}}{\partial x_{j*}} \right) = -\frac{\partial \rho_*}{\partial x_{i*}} - \rho_* \frac{g \cdot \partial a_*}{v_0^2 \partial x_{i*}} + \frac{\eta_0}{\rho_0 v_0}\,.$$

The voltage component of viscous origin in the direction Ox [19]:

$$\varsigma_{ij}{}^{*} = \eta_{*}\left(\frac{\partial v_{i*}}{\partial x_{j*}} + \frac{\partial v_{j}{}^{*}}{\partial x_{i*}}\right) - \frac{2}{3}\eta_{*}\frac{\partial v}{\partial x},$$

where the first term is the normal load, tangential second effort (the first index indicates which axis is perpendicular to the surface considered and which contains the tangential force and the second indicates the direction of force), and expresses the state of deformation. Heat equation is

$$\rho_{*}\frac{d\theta_{*}}{dt_{*}} = \frac{v_0^2}{c_m\Delta\theta_0}\frac{d\rho_{*}}{dt_{*}} + \frac{\eta_0}{\rho_0 v_0 A}\frac{v_0^2}{c_m\Delta\theta_0}\phi_{*} + \frac{\lambda_0}{\eta_0 c_m}\frac{\eta_0}{\rho_0 v_0 A}div\left[\lambda_{*}grad(\theta_{*})\right], \quad (1)$$

where: ϕ_{*} is a function of dissipation (the power dissipated by thermodynamic irreversibility); c_m is the heat mass of the fluid at constant pressure. Assuming, that the heat transfer of the law *Fourier* [7], [8], [11]:

$$q = -\lambda grad\theta,$$

where q is the heat flux crossing an area dS (vector normal to the surface S), then heat flow as the direction Ox, will be $q_i n_i dS$.

Molecular diffusion equation constituent fluids (Fick's law), expressing the process of molecular diffusion or exchange of substance, is

$$\frac{\partial c_{*}}{\partial t_{*}} + div(c_{*}v_{*}) = \frac{B}{Av_0}div\left[grad(c_{*})\right] = \frac{B}{v}\frac{v}{Av_0}div\left[grad(c_{*})\right] \quad (2)$$

(cinematic viscosity ofvthe report was noted with fluid), and the B diffusion coefficient.

The equation of state of the fluid is $\rho_{*} = f(\rho_{*}, \theta_{*}, c_{*})$.

For concentration and temperature fluctuations within the volume studied, assuming a specific mass independent of pressure, equation of state can be developed in Taylor series and retain only the first terms

$$\rho(\theta_0 + \Delta\theta, c_0 + \Delta c) = \rho(\theta_0, c_0) + \Delta c\frac{\partial\rho}{\partial c} + \Delta \Leftrightarrow \rho = \rho_0 + \Delta\theta_0\left(\frac{\partial\rho}{\partial\theta}\right)_0 + \Delta c\left(\frac{\partial\rho}{\partial c}\right)_0,$$

where: c_0 pollutant concentration in the fluid is brought to the input carrier and $\rho_0(\theta_0, \chi_0)=\rho_0$, is the initial density of the fluid.

Given that the term $-\frac{1}{\rho_0}\left(\frac{\partial\rho}{\partial\theta}\right)_0$, is the coefficient of thermal expansion β, and dividing the previous term relationship ρ_0, obtain

$$\frac{\rho}{\rho_0} = 1 - \beta\Delta\theta + \frac{\Delta c}{\rho_0}\left(\frac{\partial\rho}{\partial c}\right)_0 \quad (3)$$

or in dimensionless coordinates

$$\rho_{*} = 1 - \Delta\theta_{*}\Delta\theta_0\beta + \frac{c_1 - c_0}{\rho_0}\left(\frac{\partial\rho}{\partial c}\right)_0 c_{*}. \quad (4)$$

Moreover, pressure p and density ρ the fluid in chamber varies along the trajectory depending on the pressure p_0 and density of the fluid brought to the entrance, so

$$\rho = \rho_0 + \rho', \; p = p_0 + p \text{ and } p_0 = -\rho_0 gA,$$

where, g is gravitational acceleration.

It will develop Taylor series derivative ratio (which occurs in the equation of motion dynamics), where Ox direction of movement of the fluid

$$\frac{1}{\rho}\frac{\partial p}{\partial x_i} = \frac{1}{\rho_0}\frac{\partial p_0}{\partial x_i} + \frac{1}{\rho_0}\frac{\partial p'}{\partial x_i} + \frac{\rho'}{\rho_0^2}\left(\frac{\partial p_0}{\partial x_i}\right).$$

In view of equation (2) and earlier expression of p_0, obtain

$$\frac{1}{\rho}\frac{\partial p}{\partial x_i} = -g\frac{1}{\rho_0}\frac{\partial h}{\partial x_i} + \frac{1}{\rho_0}\frac{\partial p'}{\partial x_i} - \left[\beta\Delta\theta - \frac{c}{\rho_0}\left(\frac{\partial\rho}{\partial c}\right)_0\right]g\left(\frac{\partial A}{\partial x_i}\right)$$

normalized shape

$$\frac{1}{\rho_{*}}\frac{\partial p_{*}}{\partial x_i{}^{*}} = -\frac{gA}{v_0^2}\frac{\partial a_{*}}{\partial x_i{}^{*}} + \frac{\partial p'}{\partial x_i{}^{*}} - \left[Ar\Delta\theta_{*} - \frac{c_1 - c_0}{Fr}\left(\frac{\partial\rho}{\partial c}\right)_0 c_{*}\right]\frac{\partial A_{*}}{\partial x_i{}^{*}},$$

in which he noted: the $Ar = \Delta\theta_0 \cdot \beta\frac{gA}{v_0^2}$, Archimedes number (expressing the ratio of mass and momentum forces of fluid flow brought on site) and $Fr = \frac{v_0^2}{gA}$, Froude's number (expressed similarity in the conditions prevailing gravitational forces).

In this context dynamic equation of motion has the form of dimensionless

$$\frac{\partial v_i{}^{*}}{\partial t_{*}} + v_j{}^{*}\frac{\partial v_i{}^{*}}{\partial x_j{}^{*}} = -\frac{\partial p_{*}'}{\partial x_i{}^{*}} + \left[Ar\Delta\theta_{*} - \frac{c_1 - c_0}{Fr\rho_0}\left(\frac{\partial\rho}{\partial c}\right)_0 c_{*}\right]\frac{\partial a_{*}}{\partial x_{i*}} + \frac{1}{\mathrm{Re}}\cdot\frac{\partial\varsigma_{ij}{}^{*}}{\partial x_j}, \quad (5)$$

in which Reynolds number Re is given by the ratio $\frac{\rho v_{0A}}{\eta_0}$, applicable in this case, since the site is low speed (air compressibility is neglected). It is noted that the continuity equation remains unchanged in shape, and the equation of

motion occurred a number of dimensionless quantities (called numbers or criteria), formed with sizes A, v_0, p_0, c_0, ..., characteristic phenomenon studied [23].

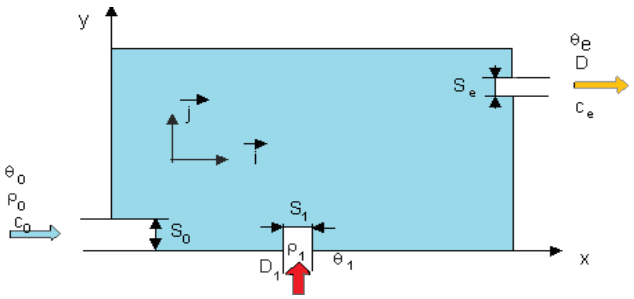

Fig.1: Explanatory sketch highlighting the conditions to limit the phenomenon of recirculation for the case of the release of harmful substances: S_0, S_1, S_e- areas to place fresh air pollutant, that pollutant exhaust-air mixture; D, D_1- mixture exhaust flows, pollutant input respectively.

B. The specific conditions of the phenomenon of recirculation (Fig.1). If it is assumed that fluid is introduced properly as long as its concentration is zero (c_0=0), then the new configuration, the limit conditions will be written [15], [21], [24]:

- to speed: $\vec{v}=\vec{0}$ wall surfaces (either $\vec{v}_*=\vec{0}$ enclosure wall surfaces);

$\vec{v}=\frac{1}{S_0}(D-D_1)\vec{i}$ entrance (or $\vec{v}_*=\vec{i}$ entrance on site);

$\vec{v}=\frac{D}{S_e}\vec{j}$ exit (or $\vec{v}_*=\frac{S_0}{S_e}\frac{D}{D-D_1}\vec{j}$ out of site); $\vec{v}=\frac{D_1}{S_1}\vec{j}$ pollutant source (either $\vec{v}_*=\frac{S_0}{S_1}\frac{D_1}{D-D_1}\vec{j}$ the source of a pollutant);

- temperature: $\theta=\theta_0$ entrance (or $\theta_*=0$ entrance on site); $\theta=\theta_e$ exit (or $\theta_*=1$ out of site); $\theta=\theta_0$ pollutant source (either $\theta_*=\frac{\theta_1-\theta_0}{\theta_e-\theta_0}$ the source of a pollutant); $\theta=g_1(x,y,z)$ the walls of the enclosure, where the coordinates x, y, z describe the wall (or $\theta_*=g_{1*}(x_*,y_*,z_*)$ the walls, where $g_{1*}(x_*y_*,z_*)$ is a function describing the wall);

- for concentrations: $c=C$ entrance (or $c_*=0$ the entry on site); $c=c_e$ exit (or $c_*=\frac{D_1}{D}$ out of site); $c=c_1$ pollutant source (either $c_*=1$ the source of a pollutant);

- for densities: $\rho=\rho_0$ entrance (or $\rho_*=1$ the entry on site); $\rho=\rho_1$ pollutant source (either $\rho_*=\frac{\rho_1}{\rho_0}$ pollutant source).

If a steady, time initial conditions are void. From equations (1), (2), (3), (4) and limit the conditions to identify the following dimensionless groups:

- $E=\frac{v_0^2}{c_p\Delta\theta_0}$, Eckert's number (expressed heat mass transfer);

- $\mathrm{Re}=\frac{\rho v_0 A}{\eta_0}=\frac{v_0 A}{v}$, Reynolds number; Pe=Re.Pr, heat Peclet's number, with $\mathrm{Pr}=\frac{\eta_0 c_0}{\lambda}$ Prandtl's number (expressed forced convection heat); Sc.Re, Peclet number of mass with $Sc=\frac{v}{D}$ Schmidt's number (expressed diffusion);

- $Ar=\Delta\theta_0\beta\frac{gA}{v_0^2}$ Archimedes number and $Fr=\frac{v_0^2}{gA}$ Froude number;

- $\frac{c_1}{\rho_0}\left(\frac{\partial\rho}{\partial c}\right);\frac{S_0}{S_1}\frac{D_1}{D-D_1};\frac{S_0}{S_e}\frac{D}{D-D_1};\frac{\theta_1-\theta_0}{\theta_e-\theta_0};g_{1*};\frac{D_1}{D};\frac{\rho_1}{\rho_0}$ (expresses geometric conditions).

Previous dimensionless groups can be used simultaneously to achieve similarity between the real situation and model, and as such, retain only those groups that characterize the phenomenon studied and serve the wording of the problem (with the release of harmful air recirculation).

It will attach indices r and m, the reference to the actual situation and the model. Scale factor of the real case (where the actual fluid is air) and the model is denoted by K, and is given by the ratio $\frac{A^{(r)}}{A^{(m)}}$. It will consider values above dimensionless groups where the model fluid is water or air.

C. The fluid in the model is water. It will study the condition Reynolds. For two movements that dominate the friction forces are also both model and in reality, it is necessary for the design Reynolds number is idem with the installation of such [10].

$$\mathrm{Re}^{(m)}=\mathrm{Re}^{(r)}$$
$$\Leftrightarrow\left(\frac{v_0 A}{v_0}\right)^{(m)}=\left(\frac{v_0 A}{v_0}\right)^{(r)}\Rightarrow\frac{v_0^{(m)}}{v_0^{(r)}}=K\frac{v_0^{(m)}}{v_0^{(r)}}$$

The temperature 20^0C, cinematic viscosity values for water and air are $v_0^{(m)}=10^{-6}\,m^2s^{-1}$, that $v_0^{(r)}=15.10^{-6}\,m^2s^{-1}$. Requiring compliance with Reynolds similarity shows $\frac{v_0^{(m)}}{v_0^{(r)}}=\frac{K}{15}$. For the influence of the type Arhimedic appearing as a result of temperature differences are idem model and reality must be respected similarity Archimedes

$$\mathrm{Ar}^{(m)}=\mathrm{Ar}^{(r)},\quad \Delta\theta_0^{(m)}\beta^{(m)}\frac{A^{(m)}}{v_0^{2(m)}}=\Delta\theta_0^{(r)}\beta^{(r)}\frac{A^{(r)}}{v_0^{2(r)}}$$

The values of coefficient of thermal expansion β, the

temperature 20 ^{0}C, water and air are 2,1.10^{-4}, that 3,4.10^{-3} [^{0}C^{-1}]. So, then the similarity *Arhimede* :

$$\mathrm{Ar}^{(m)}=\mathrm{Ar}^{(r)} \Leftrightarrow \frac{\Delta\theta^{(m)}}{\Delta\theta^{(r)}}=\frac{\beta^{(r)}}{\beta^{(m)}}\frac{A^{(r)}}{A^{(m)}}\frac{v_0^{2(m)}}{v_0^{2(r)}},$$

A report of the temperature variation model and the real case is $\frac{\Delta\theta^{(m)}}{\Delta\theta^{(r)}}\cong\frac{K^3}{15}$ (whether the condition of similarity and Reynolds). Similar climatic condition expressed by Ar, idem in kind and the model is difficult to meet in practice (if the scale factor is 20, where temperature variation is real 10 ^{0}C, and then the model should be a temperature difference of 5,3.10^3!!!).

D. The fluid model is air. The similar climatic conditions, expressed by Re idem and Ar idem are the same. As described above, the condition of similarity Ar idem is difficult in practical terms, leading to the conclusion that incompatibility condition appears between Reynolds and Archimedes condition that can not be satisfied simultaneously.

It was shown that Reynolds number does not intervene in the laws above a certain critical value (use the field of forging, which means certain conditions of production of phenomena in nature and the model).

Reynolds similarity is $\mathrm{Re}>\mathrm{Re}^{(m)}_{critic}$ the model, and $\mathrm{Re}>\mathrm{Re}^{(r)}_{critic}$ for real. It is assumed that for such values of Re number, density and temperature flow field are much higher flux density of matter and temperature caused by molecular diffusion. This hypothesis is to remove the similarity of mass and heat Peclet's (used hydraulic distortion, which means a waiver of the conditions of similarity in the area where it does not influence the shape of the phenomenon).

If the model will work at constant temperature (Archimedean condition is removed), then the remaining dimensionless groups will be (completely determined way phenomenon):

$$1)\ \frac{c_1}{\rho_0}\left(\frac{\partial\rho}{\partial c}\right)_0;\quad 2)\ Fr=\frac{v_0^2}{gA};\quad 3)\ \frac{S_0}{S_1}\frac{D_1}{D-D_2};$$

$$4)\ \frac{S_0}{S_e}\frac{D}{D-D_1};\quad 5)\ \frac{D_1}{D};\quad 6)\ \frac{\rho_1}{\rho_0}.$$

Ensure cinematic similarity requires Reynolds conditions in addition to the actual layout and where and the conditions of geometric similarity [22], [23]:

$$\left(\frac{S_0}{S_e}\right)^{(r)}=\left(\frac{S_0}{S_e}\right)^{(m)};\quad \left(\frac{S_0}{S_1}\right)^{(r)}=\left(\frac{S_0}{S_1}\right)^{(m)}$$

The similarities noted above (3), (4) and (5) are equivalent, and so keeping the equality of real and model is reduced to dimensionless groups:

$$a)\ \frac{c_1}{\rho_0}\left(\frac{\partial\rho}{\partial c}\right)_0;\ b)\ \frac{v_0^2}{gA};\ c)\ \mathrm{Re}>\mathrm{Re}_{critic};\ d)\ \frac{\rho_1}{\rho_0}\ ;\ e)\ \frac{D-D_1}{D_1}$$

The latter system consists of five dimensionless groups, determine the full deployment of the phenomenon of recirculation, without the need of the whole set of equations and conditions written at the beginning of the paragraph.

E. Results. The question is: what values are climate variables in model, if you use water as a carrier fluid (clean)?

For an actual configuration of a site (Fig. 2), scale layout will be (for a scale factor K=20): $A^{(m)}$=140 mm-height layout; $A_0^{(m)}$=260 mm - length layout; A_1(m)=180 mm - width layouts.

From the condition of similarity (e)

$$\left(\frac{D-D_1}{D}\right)^{(m)}=\left(\frac{D-D_1}{D}\right)^{(r)},$$

pollutant flows will result (D_1(m)=0.5 l.min^{-1}), and the carrier fluid ($D^{(m)}$=6.71 l.min^{-1}). Condition (b) Froude number similarity requires that the model is equal to the Froude number for real

$$\frac{v_0^{(r)}}{gA^{(r)}}=\frac{v_0^{(m)}}{gA^{(m)}}\Rightarrow v_0^{(r)}=\frac{(D-D_1)^{(r)}}{S_0^{(r)}}=0.514ms^{-1},$$

$$v_0^{(m)}=\frac{v_0^{(r)}}{K}=0.115ms^{-1},$$

where, $(D\text{-}D_1)^{(m)}$=6.21 l.min^{-1}, resulting from the condition of similarity (b). It must be met the condition of similarity both real and model case (c). Reynolds number if the model is real and 96000, respectively 16,100. To calculate the ratio $\frac{\partial\rho}{\partial c}$, which appears in similar condition (a). There are two situations.

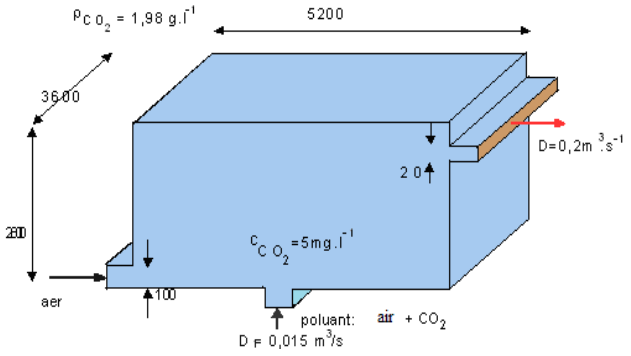

Fig. 2: Dimensions in [mm], the actual configuration of a room.

1) If the pollutant is a gas mixture between a carrier fluid and an indicator of pollutant toxic (non-reactive mixture).

To determine the density $\rho(c)$ concentration when the fluid index is c [g.l^{-1}], will be considered: one liter of pollutant consisting of a mass of toxicity indicator ρ_1, and a carrier fluid with mass of ρ_0.

Noting with V_1, specific volume occupied by toxic indicator, the resulting mass balance equation [20]

$$\rho(c)=\rho_0(1-V_1)+\rho_1 V_1,$$

where:

$$\rho_1=\frac{c}{V_1}\Rightarrow\rho(c)=\rho_0\left(1-\frac{c}{\rho_1}\right)+c.$$

By derivation with respect to concentration c, resulting relationship for calculating final $\frac{\partial\rho}{\partial c}=1-\frac{\rho_0}{\rho_1}$, that can be used when the pollutant is a gas mixture.

2) If the pollutant is an aqueous solution. If c[g.l^{-1}], is the concentration of a weak aqueous solution, then it is allowed the relationship

$$\rho(c)=a(1+bc),$$

where, through differentiation with respect to concentration c, is obtained

$$\frac{\partial\rho}{\partial c}=ab,$$

with a and b coefficients of proportionality. If the pollutant is a salt water solution as the previous relationship, is obtained $\frac{\partial\rho}{\partial c}=0.693$.

Since the imposition of similar condition (a)

$$\left(1-\frac{\rho_0}{\rho_{CO_2}}\right)\left(\frac{c_1}{\rho_0}\right)^{(r)}=0.693\left(\frac{c_1}{\rho_0}\right)^{(m)},$$

resulting value of the concentration of pollutants in the model ($c_1^{(m)}$=2.13 g.l^{-1}).

To simulate the phenomenon of recirculation, was chosen for the carrier fluid, pure water and the salt water pollutant (H_2O+KCl), with mass of 0.9996 g.l^{-1} and the temperature 20 ^{0}C, obtained

$$\left(\frac{\rho_1}{\rho_0}\right)^{(m)}=1.0014,\quad\left(\frac{\rho_1}{\rho_0}\right)^{(r)}=1.0015.$$

III. DESCRIPTION OF EXPERIMENTAL FACILITY

Using electrochemical metrology for measuring the variables of site required the use of nonmetalic materials for discharge pipes, exhaust, etc. layout [18].

The assembly of experimental facility is outlined in Fig.3. A flow of pure water, which contains a reservoir RE1, a electric pump P2, with the discharge pipe of a tap R2 and CR2 AP watermeter used to measure water flow. A circuit saltwater tank containing a RE4, equipped with a tap R4 type all or nothing (open valve correspond to the time of introduction of pollutant in the model, triggering signal acquisition).

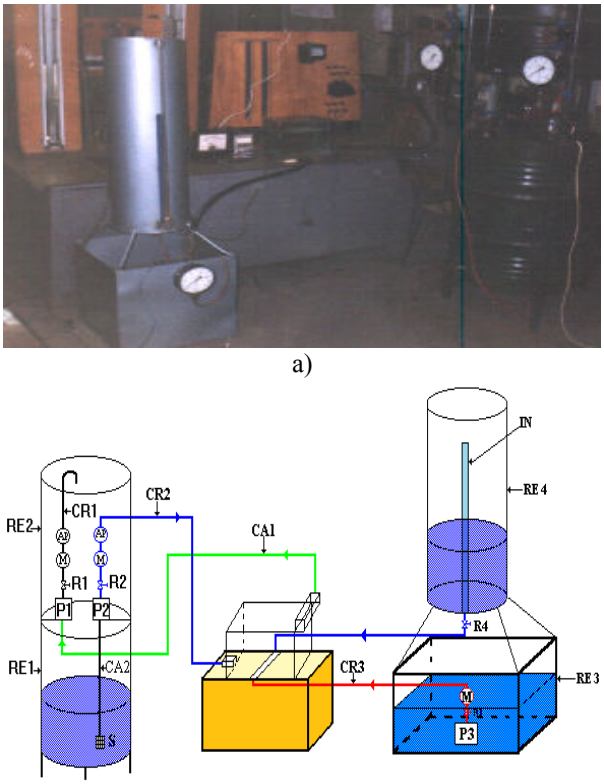

Fig. 3: Experimental installation: a) basic view b) outlined.

Fluid flow model is performed in the tank falls, the flow rate achieved by dropping the same as they flow submersible pump P3 electric pump R3 valve open. A second flow of pure water, each time allowing the replacement of salt water flow with a flow of pure water.

The circuit is composed of submersible electric pump P3 provided by CR3 discharge pipe valve R3. Rectangular tank (aquarium type) with constant level entrance equipped with a device management agent work, it can be replaced when the pure water (tap R3'), where the salt water (R4) A discharge circuit containing a P1 electric pump circuit identical to that of pure water, with the discharge pipe CR1 a tap R1. Simplified model corresponds to the pattern of air-conditioned enclosure part (Fig.4). Measurements are performed in median. Disturbance generated by placing the probe in the electrolyte is neglected and the signal from the conductometer is counted by a digital voltmeter [16].

For a scale factor equal to 20, following Reynolds similarity is obtained by introducing a flow of fluid around 7,5 l.min^{-1}. As the allure concentration after a negative step signal type tends asymptotically to zero (experimental concentration evolution can not register in time forever) will stop measuring time $t=nT_0=n\frac{V}{D}$, n>1. Flow

D=7,5 l.min^{-1}, time constant T_0=52 s şi n=4, During the interruption will be 208.

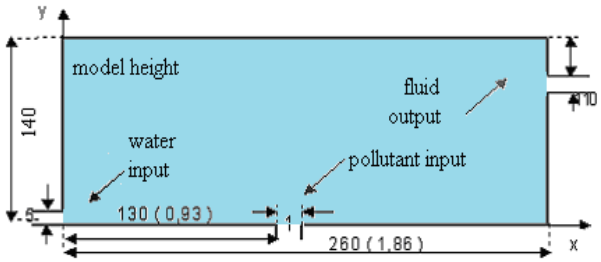

Fig. 4: The absolute values (in mm) and the normalized coordinates (on height) of the model.

IV. MEASUREMENT OF CLIMATE VARIABLES FROM THE PLANT

A. The principle of conductometer method. Where is denoted by γ, specific conductivity of electrolyte and its concentration c, it was shown that for a weak solution of potassium chloride (KCl), the temperature 20 ^{0}C There is relatively $\gamma = 1{,}636 \cdot 10^{-3} \left[\Omega^{-1} cm^{-1}\right]$. By applying a voltage electrolyte (Fig. 5), the current through the circuit is representative of the concentration of the electrodes.

The electrolyte can be characterized by parameter k, defined as the product between the average strength of the solution in volume measurement and its specific conductivity $k = R\gamma\left[cm^{-1}\right]$. It also shows that, 90% the measured conductance comes from a volume measure equal to $2{,}11.k^{-3}$, surrounding the microelectrode. Measuring system, consisting of an electric power source E-microelectrode an electrode pair placed in a saline solution, Ohm's law in the complex is

$$\underline{E} = (Z + r)I \Rightarrow \underline{U}_0 = r\underline{I} = \frac{rE}{Z + r},$$

where R is the resistance measuring device; U_0 is the voltage at the terminals of the measuring device, I is currently travelling the circuit, Z is the impedance of all electrode-electrolyte solution, having a complex value

$$Z = R - \frac{j}{2\pi f C_E},$$

where: f is frequency alternating signal; C_E capacity is equivalent capacity C_1, C_2 arising between the electrodes and solution (Fig.5b).

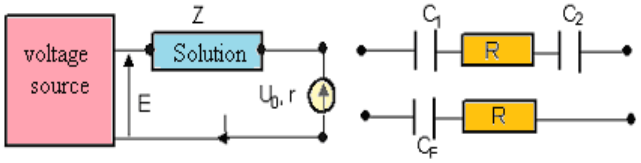

a) b)

Fig. 5: Explanatory system of measurement used for determining the concentration of: a) diagram of the system, b) diagram of all electrode-electrolyte solution.

Measuring current I, through the salt solution is carried out through a conductometer hole. In practice, the measured voltage is a rectified voltage as reactants value has an low order of magnitude ($\approx 10^3 \Omega$), average resistance to saline ($\approx 10^5 \Omega$). Since the average resistance value of the solution is approximately $5.10^5 \Omega$ (obtain $|Z| \cong R$), and the resistance value measuring device is much smaller than the average strength of the solution (r<<R), voltage measured U_0 is proportional to the concentration

$$U_0 = \frac{rE}{R + r_0} = \frac{rE}{R} \Rightarrow U_0 = 1{,}636 \cdot 10^{-3} \frac{rE}{k} c .$$

It was studied the influence of the sampling period, there were eliminated noise from transient concentration curves (a math procedure), and were checked the quality of results obtained in the stationary phase and using the conductometer method [14], [19].

The conclusions were: a strong uncertainty in the lower region of the layout (amended by measuring flow D and D_1), and a relative uncertainty of the order of 5%, the rest of the layout (once the location of measurement point), in attempts to reproduce the measurements of phase, not taken into account the uncertainty of measurement given concentration at the bottom of the layout, which gave rise to systematic errors, there is a strong uncertainty in the evolution of concentration, because, first, the calculation is made on a limited number (11), and secondly there was no filtering to eliminate noise [12], [13].

B. The calibration of the concentration measurement system. It has been done in two stages: the first corresponds to probe-conductometer calibration unit, which allows the concentration c, if known voltage value U_0 (Fig. 6a), and the second step is to measure electrolyte parameter k, where it determines the measure. Thus, knowing the value of the device resistance R (680 Ω), and replacing the electrolyte solution through a resistor of value R, equal to the average strength of the solution, we obtain the measured blood $U_0 = \frac{rE}{R}$, which are plotted in Fig.6b. Knowing report $\frac{rE}{k}$, and product rE, can be parameter value electrolytic k. It has been obtained k=70 cm^{-1}, and volume measurement equal to 6,15.10^{-6} cm^3. The relationship between instantaneous concentration c (Fig.6a), and measured voltage U_0 in terms of a model is linear c=aU_0+b. Noting the average concentration of the fluid discharged by $\overline{c_e} = \frac{1}{n}\sum_{i=1}^{n} c_e(t_i)$, its associated medium voltage (measured at the pump discharge outlet P2) with $\overline{U}_e$, and average voltage measured in pure water (the concentration is zero) with $\overline{U}_1$, then for calculating the concentration at a point in the model results

$$\bar{c}_e = a\bar{U}_e + b \quad \text{and} \quad 0 = a\bar{U}_1 + b \Rightarrow \frac{c}{c_e} = \frac{U_0 - \bar{U}_1}{\bar{U}_e - \bar{U}_1}.$$

Tensions $\bar{U}_1$ şi $\bar{U}_e$ should be measured regularly because the probe response time varies. Complete determination of the error was not possible. As such were made the following assumptions: the error is negligible because the probe positioning, probe does not disrupt the flow of fluid in the model [17].

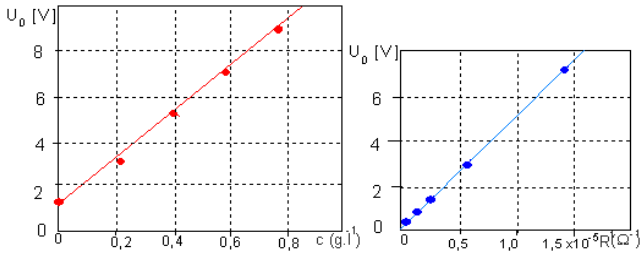

Fig. 6: Approximative curves used for calibrating of the concentration.

V. HYDRAULIC MODELLING OF THE PHENOMENON

A. Getting deterministic test signals. On the experimental application of an impulse response is difficult to obtain, whereas fluid placed in a very short time, but enough to be detected with good precision the concentration [1].

Step signals are obtained by applying a flow of fluid into experimental model, and allow pure water is monitoring developments or model of salted water. Applying a positive step signal experimental fluid means:

- At time t=0, is inserted into water will circulate in the layout a constant flow of fluid (pure water indicate progress), opening the valve R3' whit R4 valve closed.
- At time t <0, the pollutant is simulated by pure water.

The open valve R3' and R4 open the valve. At time t=0, is replaced by pure water flow through an equivalent flow of salt water, the flow dynamics will be affected but only the distribution of concentrations (salt water) will evolve. Applying a negative step signal experimental fluid means:

- At time t=0, stop the fluid injection experiment (pure water) in water entering the model. Close the valve R3'.
- At time t=0, the flow of salt water is replaced by an equivalent flow of pure water, moving only the distribution of concentrations. Close the valve opens the valve R4 and R3'.

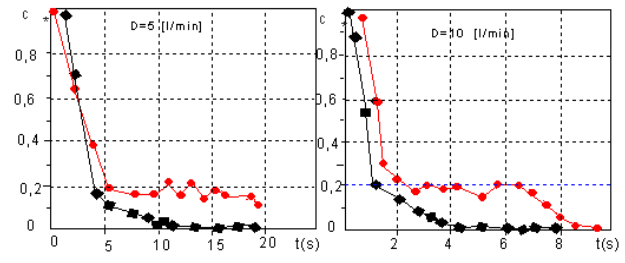

a) b)

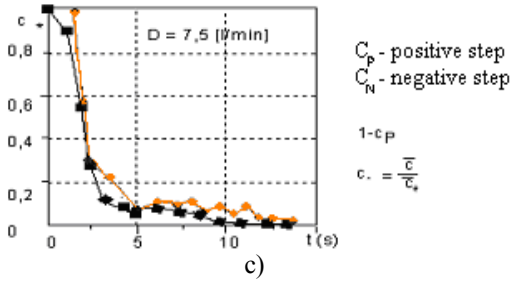

c)

Fig.7: Approximate shape of the system response for application of positive and negative step signal of pure water.

C_N – positive step When applying a step signal of pure water were represented (Fig.7), for three flow regimes, such forms of response signals a positive step (c_P) and negative (c_N), measured at the exit fluid the suction pipe CA1. When applying a step signal saltwater (pollutant) is not possible to study the response signal from the stage of pollutant emission section, the pollutant is transported only if the fluid emitted carrier (pure water) has a thickness of order of millimeters.

B. Checking the assumption of approximating the fluid flow model with a linear system. It showed that one of the conditions that allow fluid flow approximation with a linear system refers to the experimental flow brought clean water, which must not interfere with the overall dynamics of the flow (it must be constant as the flow D_1). Concentration $c(t)$ can be considered as response to a signal $x(t)$, which is applied to the entry of a linear system F (Fig. 8a).

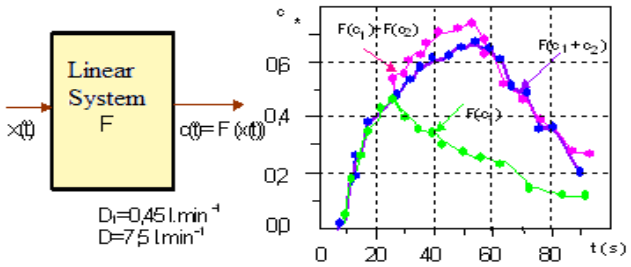

a) b)

Fig.8: Explanatory Notes on the approximation of a linear system: a) defining a linear system, b) concentration contour shape for property verification of superposition, where D_1 is brought pure water flow and D is the flow of salt water exits.

Of the three properties characteristic of a linear system:
a) the property of superposition [2], [3]

$$F[c_1(t) + c_2(t)] = F[c\ (t)] + F[c_2(t)];$$

b) the proportionality property $F[k_0 c(t)] = k_0 F[c(t)]$;

c) the property of translational invariance by temporal $\frac{F[k_0 c(t)]}{k_0 c(t)} = \frac{F[c(t)]}{c(t)}$, experimental system is enough to check only the first two.

To verify the first property (Fig.8b), experimental system configuration is the following:

- Insert an instant flow of pure water with concentrations c_1 and vertical profile of concentration traces normalized concentration through out $F(c_1)$; allure concentration $F(c_1)$ decreases from t=24 s, repeat the previous operation, introducing the time t=24 s a new flow of pure water with concentrations c_1 and vertical profile of concentration traces normalized $F(c_1) + F(c_1)$;
- To introduce a flow of pure water instantly concentration $2c_1$, and assigns the vertical concentration profile normalized by the concentration of exit $F(c_1 + c_1)$.

There is a satisfactory overlap of the curves $F(c_1+c_1)$ and $F(c_1)+F(c_1)$. To verify the second property, the system configuration is as follows: c_1=0,65 g.l^{-1}, c_2=k_0c_1=2,5 g.l^{-1}, D=7,5 l.min^{-1}, D_1=0,3 l.min^{-1}.

They have been drawn the vertical profiles of the concentration normalized by the exit concentration (Fig.10) upstream of the first profile is the emission slit flow of pure water (Fig. 9a), and the next downstream (Fig. 9b).

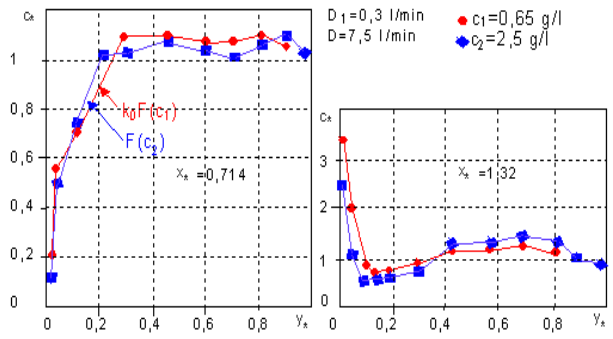

a) b)

Fig.9: Approximate shape of concentration curves for verifying ownership of proportionality: a) upstream transmission slot, b) downstream of the emission slit.

There is a good overlap of normalized concentrations profiles. It also notes the existence of significant deviations downstream of introducing pure water surface (the first two values of the profile Fig. 10b).

The results were obtained spreadsheet and then plotted in both cases. Similarity in a fluid flow chamber with an air-conditioned linear system, using the input signals of fluid experimental stage, seems to be a reliable method to characterize the air conditioning on site.

C. Influence of reynolds number on flow in the model (*disturbance on the process*). Knowing the concentration distribution function of Reynolds number provides information on proper disposal of pollutant in the model (indicate the area where the pollutant comes). Different flow regimes and thus different values of Reynolds number are obtained for different positions of the valve R2.

Results in stationary regime. He studied the evolution of concentrations in a median of five values as the Reynolds number: 6920, 12960, 19440, 25930, 44070. Results obtained in steady, indicating two types of configurations: Re=6920 (Fig.10) şi 12960≤Re≤54440 (Fig.11, Fig.12). For the Reynolds number equal to 6920, approximately vertical profile of concentration has two features.

a) Plan of action is located upstream of the surface emission of pollutant ($0.0036 \le x^* \le 0.36$).

In this situation, first normalized concentration is low (c^*=0.05), then salt abruptly to a value close to 1 (the concentration becomes uniform on site, the same value with the exit of the site).

b) action plan is in the range: $0.71 \le x^* \le 1.82$. In the beginning, has high levels normalized concentration (c^* =10), then decreases rapidly.

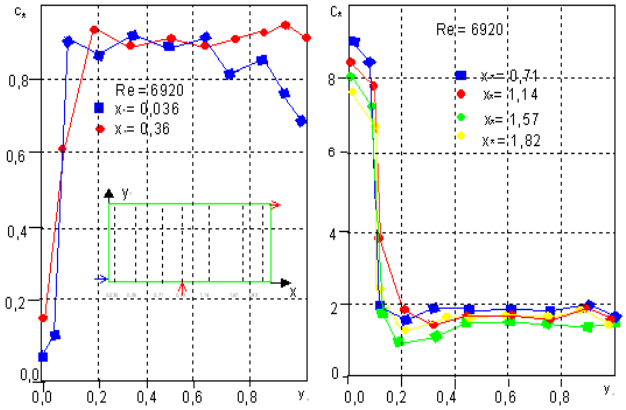

Fig.10: The approximative vertical profile of the concentrations.

The peculiarity of this configuration is that two types of profiles are concentrations of a side surface of the pollutant emission located at x^*=0.929. It highlights the absence of convection (movement of whole particles fluid upward dynamic in nature) in the emission of pollutant molecular diffusion provides pollutant transport, so that the influence of water flow is not showing. It was noted, in terms of concentration Profiled appearance of stratification phenomenon, because the difference between fluid density and pollutant carrier (which is the order of 2 g.l^{-1}).

Resuming experience, and using coloured water to simulate pollutant (whose density is very close to that of pure water), it was observed that the stratification phenomenon disappeared.

For Reynolds numbers within the range (12960 ... 44070), Profiled normalized concentrations (Fig.11 and Fig.12), taking into account the measurement uncertainty due to become independent of Re.

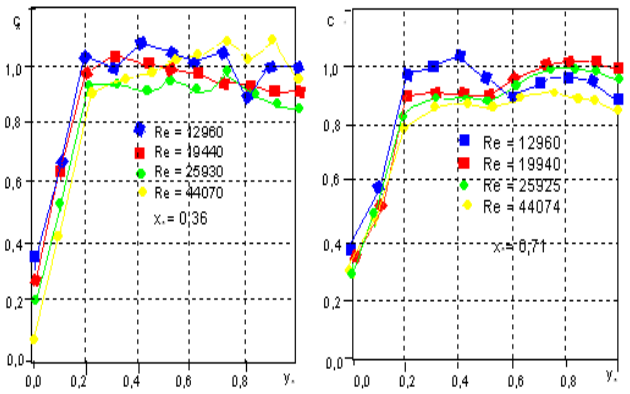

Fig.11: Approximately vertical profile of normalized concentrations upstream the slot of the pollutant emission.

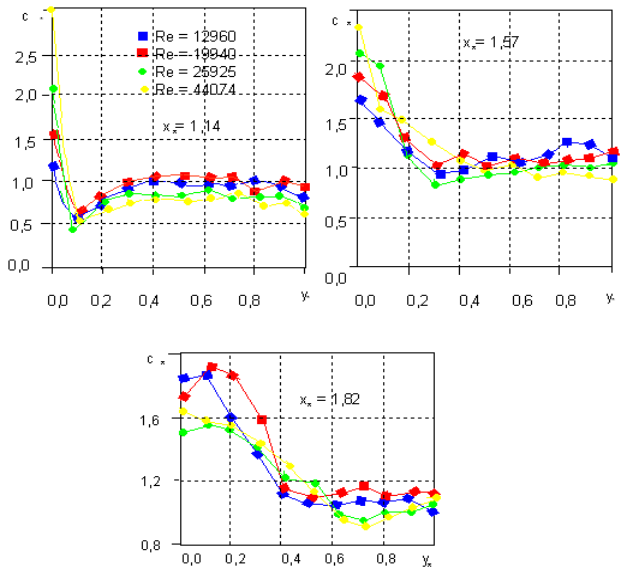

Fig.12: About the vertical profile concentrations downstream of the pollutant emission slot.

VI. HYDRAULIC SIMULATION

A. Results in phase. If the concentration and fluid velocity is decomposed into a sum of an average part and a fluctuating $c=\bar{c}+c',v_i=\bar{v}+v_i'$ and if density effects are neglected, and assumes an isotropic turbulence, where molecular diffusion equation (2) becomes

$$\frac{\partial \bar{c}}{\partial t}+\bar{v}_i\frac{\partial \bar{c}}{\partial x_i}=\frac{\partial}{\partial x_i}\left(B\frac{\partial \bar{c}}{\partial x_i}\right) \qquad (6)$$

The dimensionless variables, highlighting the indirect method of analysis $c_*=\frac{\bar{c}}{\bar{c}_e};t_*=\frac{t}{\tau_e};\bar{v}_i^*=\frac{\bar{v}_i}{v_0};\ x_{i*}=\frac{x_i}{A_0}$, where: $\bar{c}_e$ is the mean concentration of fluid in the fluid extracted experimentally, τ_e age carrier fluid extract, v_0 is the horizontal velocity of the fluid carrier introduced $A_0=v_0\tau_e$ is the length of the layout. Previous equation arises as dimensionless

$$\frac{\partial c_*}{\partial t_*}+v_{i*}\frac{\partial c_*}{\partial x_{i*}}=\frac{\partial}{\partial x_{i*}}\left(\frac{B}{v_0^2\tau_e}\frac{\partial c_*}{\partial x_{i*}}\right). \qquad (7)$$

Assuming a steady concentration of $\frac{\partial c_*}{\partial t_*}=0$, and assuming that the phenomenon of diffusion is independent of time, we obtain :

$$v_{i*}\frac{\partial c_*}{\partial x_{i*}}=\frac{\partial}{\partial x_{i*}}\left(\frac{B}{v_0^2\tau_e}\frac{\partial c_*}{\partial x_{i*}}\right).$$

If an identical flow, both for speed and average concentrations, the report $\frac{B}{v_0^2\tau_e}$ is independent of Reynolds number, which implies, if one takes into account the equation (7), a normalized concentration $c_*(t_*)$ independent of Reynolds number values. Integrating equation (6) with respect to time, where the flow is stationary for speed, we obtain:

$$\int_0^\infty\frac{\partial \bar{c}}{\partial t}dt+\int_0^\infty\bar{v}_i\frac{\partial \bar{c}(t)}{\partial x_i}dt=\int_0^\infty\frac{\partial}{\partial x_i}\left(B\frac{\partial \bar{c}}{\partial x_i}\right)dt \qquad (8)$$

Assuming that at time t=0, the signal a negative step experimental fluid (indicator), equation (8) will take the form:

$$-\bar{c}(0)+\bar{v}_i\frac{\partial}{\partial x_i}\int_0^\infty\bar{c}dt=\frac{\partial}{\partial x_i}\left[B\frac{\partial}{x_i}\int_0^\infty\bar{c}dt\right], \text{ or, if}$$

account is taken of how to define the internal age of the experimental fluid $\tau_i=\frac{1}{\bar{c}(0)}\int_0^\infty\bar{c}(t)dt$, then

$$-\bar{c}(0)+\bar{v}_i\frac{\partial\left(\bar{c}(0)\tau_i\right)}{\partial x_i}=\frac{\partial}{\partial x_i}\left[B\frac{\partial\left(\bar{c}(0)\tau_i\right)}{\partial x_i}\right].$$

The normalization is obtained

$$-c_*(0)+v_{i*}\frac{\partial\left(c_*(0)\tau_{i*}\right)}{\partial x_{i*}}=\frac{\partial}{\partial x_i}\left[\frac{B}{v_0^2\tau_e}\frac{\partial\left[c_*(0)\tau_{i*}\right]}{\partial x_{i*}}\right]. \qquad (9)$$

If the flow is identical (similar) for speed and average concentrations of equation (9) is inferred that when the flow rate is independent of input v_0 fluid carrier and the product $c_*(0)\,\tau_{i*}$ (or age τ_{i*}) is independent of Reynolds number. So, if a flow is similar to average speed and concentration, then reports $\frac{\bar{c}}{\bar{c}_e}\left(\frac{t}{\tau_e}\right)$ and $\frac{\tau_i}{\tau_e}$ are independent of Reynolds number. If the report $\frac{\tau_i}{\tau_e}$, is independent of Reynolds number means that the same degree report $\frac{\langle\tau_i\rangle}{\tau_e}$ is independent of Reynolds number. It will calculate reports $\frac{\langle\tau_i^F\rangle}{(\tau_e)_m}$, $\frac{\tau_i^P}{(\tau_e)_m}$ and $\frac{\langle\bar{c}\rangle}{\bar{c}_e(0)}$ and will pass in Table 1 (indices *m, F* and *P* are reference to the measured values of fresh fluid and pollutant).

Tab.1: Reynolds number influence on climate variables from the plant.

Re	$\frac{\langle\tau_i^F\rangle}{(\tau_e)_m}$	$\frac{\tau_i^P}{(\tau_e)_m}$	$\frac{\langle\bar{c}\rangle}{\bar{c}_e(0)}$
6.920.	0,95	0,84	0,94
12.960.	0,94	0,84	0,87

19.440.	0,98	0,88	0,91
25.930.	0,98	0,90	0,88
35.000.	0,98	0,88	0,91
44.070.	0,97	0,77	0,87
54.440.	0,96	0,72	0,86

Figure 13 compares the evolution of transient curves $\frac{c_e^{-F}(t)}{c_e^{-F}(0)}$ and $\frac{c_e^{-P}(t)}{c_e^{-P}(0)}$ for different Reynolds numbers. There is a fairly good overlap of curves for a number Re, between 25930 and 55440. However, the distribution of concentration allowed the definition of three regions.

The first region corresponds to the entry area of the fluid carrier in the model, and is characterized by a low concentration (less polluting). The outline of this region is the first moments of the inferior wall layout, after which the right of the pollutant emission surface rises slightly (Fig.14).

The second region corresponds to an expansion of the area of pollution, building on the surface of pollutant emission, and is characterized by high pollutant concentration values. Therefore, in this region influence pollutant introduced fluid is more apparent. You can not know exactly where the substance transport is by diffusion or convection.

The third region is characterized by a concentration of values about equal to 1, and represents a substantial amount of makeup. If it is desired to distinguish the specific flow inside the layout, will be considered internal age (life) of fluids.

B. Estimating the efficiency of air conditioning with internal age. Age study internal fluids (pure water and salt water) the model is necessary for several reasons.

1) For the Reynolds numbers within the range [12960, 44070], it was seen that there is a region where the concentration is normalized around the value 1. Just study the internal age will allow to discern certain sub-regions within the layout of different qualities of air.

2) The results obtained have shown steady if the process of pollution in the region was of type 2 convection or diffusion, internal age of the fluid can provide such information. For flows D=7,5 l.min^{-1} and D_1=0,45 l.min^{-1}, measurements were made for the 13 points as the model: 13 for fluid carrier, and 13 for fluid pollutant.

The first points are located at the bottom of the layout (measuring points 1, 2, 3 and 4-n upstream and downstream of the pollutant emission area), and corresponding work area where people are. The following three points are located at half height layout (measuring points 6, 7 and 8), corresponding to the area where it is assumed that the pollutant would accumulate.

The following three points at the top of the layout (the points of measurement 10, 11 and 12), corresponding area in which may be a fluid recirculation. The last three points are located at corners layout (5 measuring points and 9), and out of fluid model (point of measurement 13). A brief analysis, the concentration values and the values of internal age site provides some information on the phenomenon of recirculation.

Lower values of the internal age 2 (Fig. 13), shows that the process of pollution in this area is not molecular diffusion. There is a clear link between the internal age distribution and distribution levels. For example, measuring points 1, 2 and 3 belonging to regions 1, are characterized by low internal fluid of age carrier (clean), on the contrary, the point of measure 4, which is characterized by a low internal age of the fluid carrier is part of Region 2.

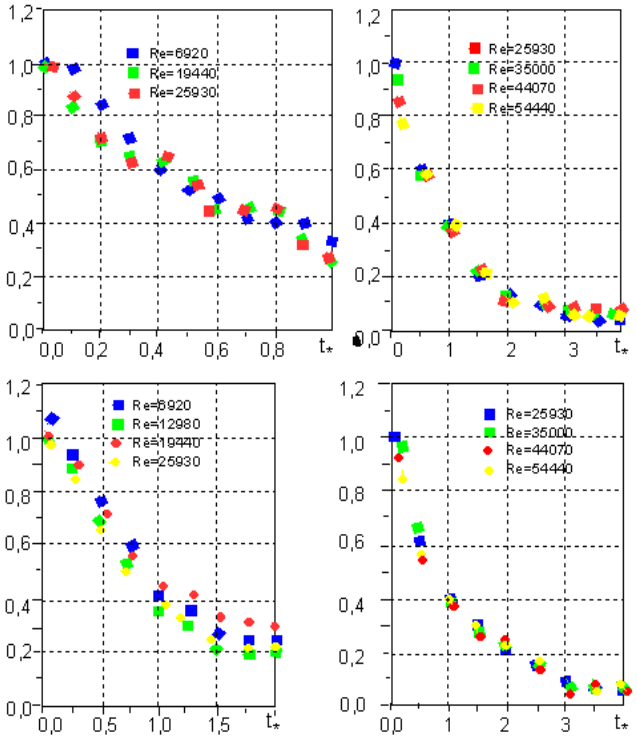

Fig.13: Answer some of the strengths (out of the model) to apply a negative step signal experimental fluid (pure water) at the entrance.

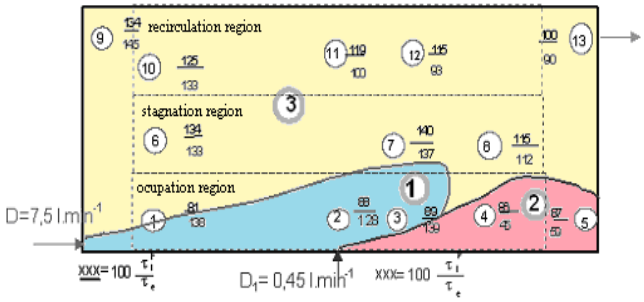

Fig.14: Position measuring points and regions, approximate values of age internal fluid model are normalized by age τ_e.

The same is observed when measured internal age of pollutant measuring points 2 and 10, belonging to different regions, have little difference whether their age is measured pollutant. In region 3, characterized by an important amount of fluid around a normalized concentration values 1, we see variations in the internal age, it is possible that points 7 and 3 have nothing in common, if it takes into account only their concentration.

The best percentage of discharges is located in the

downstream region of the pollutant emission surface (points 4 and 5) and the least good in paragraphs 1, 2, 3, 6, 7 and 9. Normalized concentration values c_* are very close to the ratio of internal age of the fluid carrier and the internal age of the pollutant (Fig. 15).

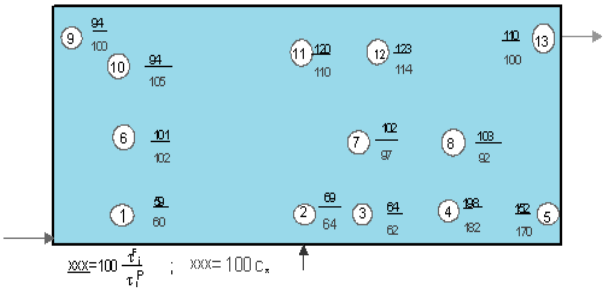

Fig.15: The analogy between direct and indirect measurement method.

Study internal age and pollutant carrier fluid can give an idea of the trajectory of these fluids on site.

C. The approximate trajectory of the fluid carrier. In the event that no diffusion occurs, the link between the concept of trajectory of the fluid and its internal age is determined assuming that two successive positions of the test response signal (impulse, step) applied at the input are characterized by increasing internal age. If it is assumed that a point of bifurcation occurs chamber fluid trajectory, then increase the internal age will be a distinct directions.

The lesser of the internal age is obtained in paragraph 1 of measurement, which is closest to the entrance and fresh fluid model. If convection were the only transport process between the entry and exit model, where internal age would be very close to zero. Arguably, the carrier fluid to reach the entry model to the point 1, in addition to convection and uses another method (diffusion).

The route will pass carrier fluid after the measuring points 2, 3, 4, 5. Then, statistically speaking right wall of the layout is fluid and fork on top of it, a part of the fluid is evacuated, and another part is recycled along the upper wall. It is difficult to make a connection between measuring point and the other 8 points (for example, points near 8 namely 7 and 12, or 7 and 4), whereas no internal age decreasing. It may, however, say that between 5 and 13 points as a fork because there is diffusion. With the departure point 10, the fluid carrier meets successive paragraphs 6 and 7, Section 9 appears to have reached the beginning of a fork, which are in the section 10 (Fig.16).

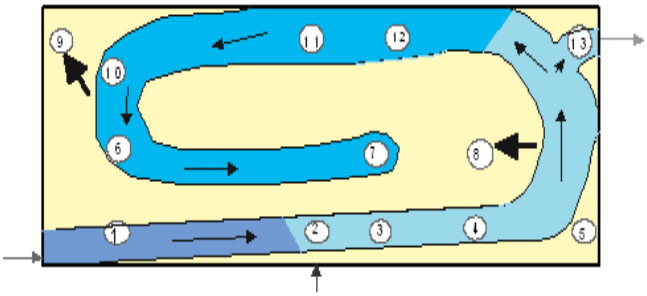

Fig.16: Approximate trajectory of the fluid carrier (clean) the model.

To establish the approximate trajectory of pollutant experimental fluid is introduced through the surface emission models, spreading it on site. The first point is the extent of pollutant reached 4 and will then, as things take place as in the case of clean fluid.

The strong analogy between the path of the pollutant and the fluid is clean because the area of emission of pollutant is located in a carrier fluid circulated enough (clean). Therefore, for an overall comparison of the trajectories of clean fluid (carrier) and the pollutant, the study sees a need for a future that would change the position of the pollutant emission. Moreover, without precise knowledge of flow dynamics, we can not say anything about internal ages of pollutant at the point of Measure 3 and 4 ($\tau_i^P(3)$ and $\tau_i^P(4)$), starting from the only knowledge about internal ages fluid clean ($\tau_i^F(3)$ and $\tau_i^F(4)$).

D. Estimating the quality of air conditioning in the model. It can be assumed that the area occupied by diluting the concentration of staff is not optimal, since the fluid recirculation inside the enclosure has the effect of pollution carrier fluid before being refreshed (see the point of measurement internal ages 3 and 4). A necessary criterion of a good air conditioning, which takes into account the behaviour and pollutant carrier fluid, such as their path does not meet the input of staff employed. Starting from the criteria of efficiency can be characterized cooling.

If the layout (Fig.17), criteria of effectiveness in a given area of model (local), the carrier fluid and pollutants will be

$$\varepsilon^F = \frac{\left\langle \tau_i^F \right\rangle}{\tau_i^F}, \qquad \varepsilon^{tr} = \frac{\bar{c}_e(0)\tau}{\bar{c}(0)\tau_i^P}$$

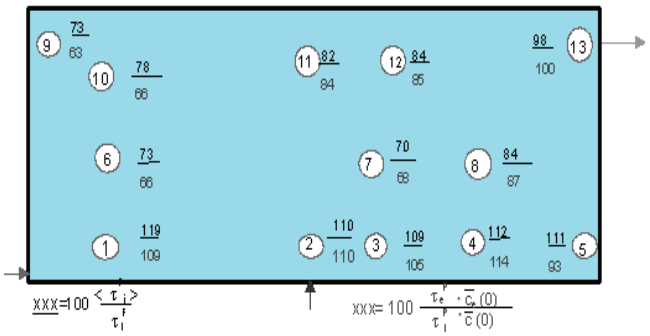

Fig.17: Approximate values of local efficiency criteria model.

Earlier it was hypothesized that the behaviour of the pollutant is similar to that of carrier fluid. So pollutant behaviour is identical to paragraphs 2 and 4.

Representing transit times t_{tr} (corresponding to the time required for the influence of the step signal to start is showing), obtained when determining the approximate trajectory of the fluid carrier and the pollutant (Fig.18), it is noted that the criterion values τ_i^F are particularly good as the transit time of carrier fluid t_{tr}^F is lower.

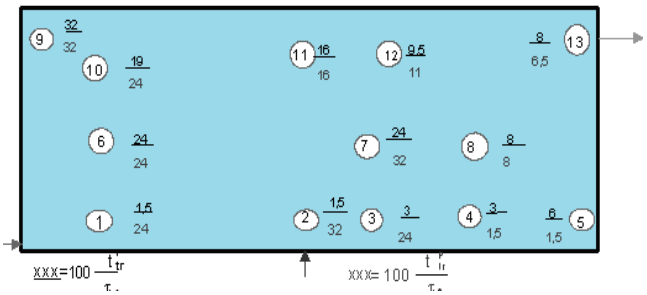

Fig.18: Approximate values of transit times in the model.

In contrast, changes in values of ε^{tr} not follow that the values of transit times for pollutant t_{tr}^{P}, and because it can provide that pollutant dilution will be less good in paragraph 4 of the layout than in paragraph 2.

E. Estimating the efficiency of air conditioning with refresh rates and escape. By applying negative fluid signals exploratory stage (when saltwater F, the water pure P) at time t=0, and representing different points of measurement for response (given the natural logarithm of the ratio of instantaneous concentration c (t) of fluid applied experimentally and concentration in the exhaust $\overline{c}_e$), will distinguish two types of evolution of concentration.

The first type of development is manifested by a rapid decrease in the concentration (in a short period of time), represented by Fig.19 with arrows, followed by a slower decrease. In this case there are points of measurement 1 (F), 10 (F and P) and 13 (F and P). As a result, the curve illustrating the evolution of concentration at negative step signal can be decomposed into two line segments.

The second type of evolution of the concentration can be compared to a single line segment, points 1 (P), 7 (F and P). If α_1 and β_2 has slopes of the first and second line segment, then the time constants T_1 and T_2 and normalized by the measured value of age carrier fluid extract $(\tau_e)_m T_i^* = 100\dfrac{T_t}{(\tau_e)_m}$, will move in Tab.2.

Calculating the ratio of standard deviation $\sigma\left(\overline{T}_{2*}\right)$:

$$\sigma\left(\overline{T}_2\right)=\sqrt{\frac{1}{n}\sum_{j=1}^{n}\left(T_{2j}-\overline{\overline{T}_2}\right)^2},$$

the 13 points of measurement (n=1..13), and their statistical average defined by the relationship $\overline{\overline{T}}_2=\dfrac{1}{n}\sum_{j=1}^{n}\overline{T}_2$, where $\overline{T}$ is the mean, dispersion is assessed by T_2:

$$\frac{\sigma\left(\overline{T}_{2*}^{=F}\right)}{\overline{T}_{2*}^{=F}}=\frac{5{,}77}{130}=4{,}4\% \quad \text{and} \quad \frac{\sigma\left(\overline{T}_{2*}^{=P}\right)}{\overline{T}_{2*}^{=P}}=\frac{9{,}64}{119}=8{,}1\%,$$

and concludes that the II part of the curve depends very least to the point of measurement chosen. It is noted that, T_1^F varies between 11,8 and 128, and that T_1^P varies between 8, 4 and 127. As a result, the value of T_{1*} is closely related to the point at which the measurement and reflects a property of flow.

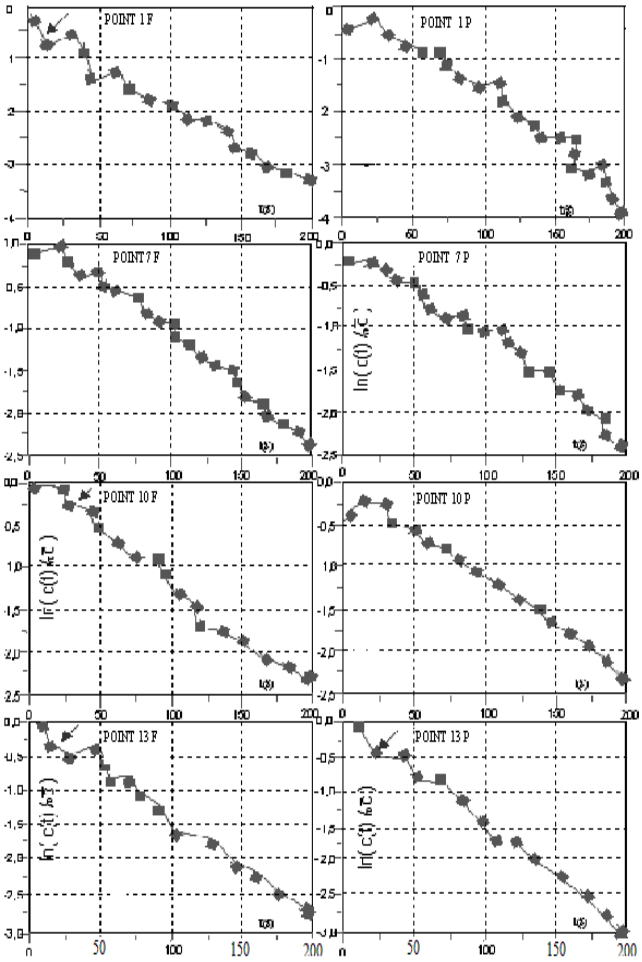

Fig.19: Logarithm of response to negative step signal at different points.

F. The average national life. In Tab.3 are given and compared the values of average lifetime internal tab.1.4 calculated using the values of the relationship:

$$T_1+(T_2-T_1)\exp(-T_0.T^{-1}_1),$$

with the value derived from steady concentration:

$$\Delta\tau = T_1+\left(T_2-T_1\right)e^{-\frac{T_1}{T}},$$

the last value is deducted directly by expressions:

$$\Delta\tau=\frac{1}{c_0}\int_t^{\alpha}c(t)dt,$$

where, $c(t)$ is the response to negative step and t is time from beginning to be felt signal (to decrease the concentration curve shape).

Values of $\Delta\tau$ (second column of Tab.3), deducted from the amount of steady concentration, and those obtained by the relationship $T_1+(T_2-T_1)\exp(-T_0.T^{-1}_1)$ (last column of Tab.3), not always close.

G. The efficiency of air conditioning. For a flow, is calculated to express the efficiency of air conditioning reports (Fig. 20),

$$\frac{\frac{1}{\Delta\tau^F}}{\frac{\tau_e}{t}} = \frac{t_*}{\Delta\tau^F} \quad , \quad \frac{\frac{1}{\Delta\tau^P}}{\frac{\tau_e}{t}} = \frac{t_*}{\Delta\tau^P} \quad ,$$

where, $t_* = \frac{t}{\tau_e}$ age is normalized value of the internal signal and $\Delta\tau^F$ and $\Delta\tau^P$ internal living environments are times when the signal is applied as a negative step, F salt water, pure water that P.

Tab.2: Approximate values of time constants at different points of measurement.

Experimental fluid injection site	Entry saltwater		Login pure water	
Time constants Points of measurement	T_{1*}^F	T_{2*}^F	T_{1*}^P	$T^P{}_{2*}$
1	11,8	134	122	122
2	18,3	140	125	125
3	17,0	138	127	127
4	20,2	138	8,4	112
5	34,7	129	15,2	122
6	128	128	114	114
7	127	127	116	116
8	80,6	127	60,5	113
9	122	122	126	126
10	62,0	131	45,0	142
11	51,2	128	32,6	103
12	38,8	122	31,0	116
13	30,2	131	27,1	113

Tab.3: The average length of the inner life of concentration response to negative step signal.

Experimental Fluid	F	P	F	P
Nr. points	$\Delta\tau$ [s]		$T_1+(T_2-T_1)\exp(-T_0.T^{-1}{}_1)$ [s]	
1	53	75	54	79
2	57	75	63	80
3	58	80	61	82
4	56	26,5	61	27,3
5	52	31	56	34,6
6	70	68	82	73
7	79	75	82	75
8	74	70	76	70
9	73	80	79	81
10	69	72	71	77
11	70	56	73	57
12	69	57	69	60
13	61	55	63	59

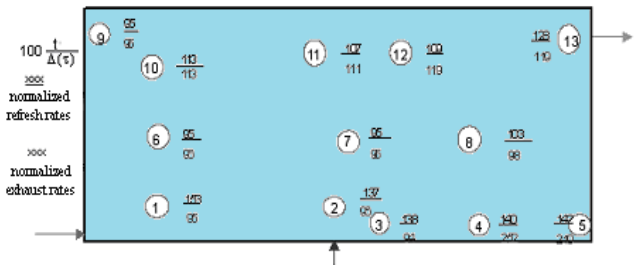

Fig.20: Approximate values of refresh rates and exhausts.

For an efficient air conditioning (in the occupation), refresh rates $100\frac{t_*}{\Delta\tau^F}$, must be close to 100. It notes that they have value: enlarge the bottom of the layout; around in the top of the layout (paragraphs 10, 11, 12), the same value in regions where domestic ages are higher (paragraphs 6, 7 and 9).

The best percentage of escape $100\frac{t_*}{\Delta\tau^P}$, are located in the downstream region of the surface emission of pollutant (items 4 and 5) and the least good in paragraphs 1, 2, 3, 6, 7 and 9.

H. Results of experimentally recirculation phenomenon.

Overlapping impulse response curves $\frac{d}{dt_*}\left(1-\frac{\bar{c}_e(t_*)}{\bar{c}_e(0)}\right)$ normalized with respect to time $t_* = \frac{t}{(\tau_e)_m}$ (Fig.21), observed that in all cases, time of occurrence of the first peak, all curves, is around values of 0.12 s.

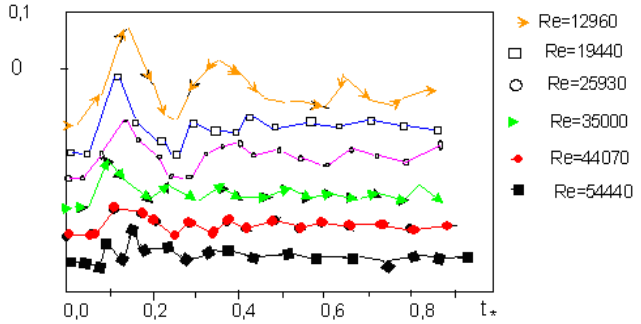

Fig.21: The answer about the momentum out of the model for different flow regimes.

VII. CONCLUSIONS

Variables that can be controlled experimental facility are: the flow of fluid evacuated, placing the fluid flow indicator, the fluid temperature and the positioning of conductometer probe. Measurement of these variables is affected by errors.

The disadvantages of the installation are caused by working in open circuit. On the other hand, is observed during the work of moving air bubbles to the top of the layout (to resume the measurements to a new steady, must wait until their disappearance). Identification operations took place in time. For the model to have a behaviour as close to the process (the error between model and process that appears to be the smallest), mean squared error was used.

The parameters obtained are optimal, as they result from minimizing an error criterion. The results show that applying a negative step signal of pure water disrupts the flow of the model less than being a positive step saltwater signal (this is why that step is preferred using negative fluid signals, and simulate the phenomenon choosing to pollutant pure water). On the one hand, we see that it is

more advantageous application of a negative step signal (response is closest to a perfect step response signal), and on the other hand, observed that the stabilization of two-dimensional flow is faster when you used to simulate pollutant pure water than salt water.

The determination of internal age carrier fluid and fluid path allows to estimate pollutant and pollutant carrier, in addition, the area alleged to be occupied by staff, the fluid is characterized by low levels of internal age, the more so as there is likelihood the fluid entered the site to be clean. Indirect method allows only a qualitative assessment of air conditioning, which is fundamental to understanding how different fluids (fluids and fluid carrier pollutant) are transported within an inside. Age law permits to have an idea (quality), the approximate trajectory of the fluid within premises. It has been seen that it would be convenient to characterize the quality of extracting the pollutant by a criterion that is to occur during transit rather than internal age.

The experimental results show that after a negative step signal fluid experimental log linear response decreases after a certain time. Furthermore the slope line is independent first point of measurement and on the other hand the place of emission of the indicator. It was also established that can characterize the response to negative step signal with the 3 values, which were used to express the refresh rate of carrier fluid and pollutant discharge. As a result, air quality can be characterized starting from the knowledge values decreasing slopes of concentration response at different points in the room, when applying a negative step signal type.

The evolution of refresh rates and exhaust values is consistent with information derived from knowledge of the internal age of the fluid.

VIII. REFERENCES

[1] Bulucea C.A., Popescu M.C., Bulucea C.A., Manolea Gh., Patrascu A., "Interest and Difficulty in Continuous Analysis of Water Quality", Proceedings of the 4th IASME/WSEAS International Conference on Energy & Environment, pp.220-225, Cambridge, February 2009.

[2] Bulucea C., Bulucea A., Popescu M.C., Cornea E., "Characterizing Biomedical Waste in Hospitals of Dolj District", EnvironmentaL Problems and Development, Proceedings of the 1st WSEAS International Conference on Natural Hazards, pp.97-104, Bucureşti, novembre 2008.

[3] Bulucea C.A., Bulucea C.A., Popescu M.C., Patrascu A., "Assessment of Biomedical Waste Situation in Hospitals of Dolj District", International Journal of Biology and Biomedical Engineering, Issue 1, Vol.2, pp.19-28, 2008.

[4] Degeratu Pr., Popescu M.C., "Linéarité du système de climatisation I", International Conference on Applied and Theoretical Electricity, Vol.III, pp.269-273, Craiova, iunie 1998.

[5] Degeratu Pr., Popescu M.C., *L'approximation, l'interprétation et la simulation numérique du débit d'air fraîche pour des pièces ou il y a des agglomérations de gens*, Anale Universitatea Constantin Brâncuşi. Editura Ager, pp.47-52, Tg.-Jiu,1996.

[6] Popescu M.C., Degeratu Pr., "Climatisation passive pour l'habitat", International conference on applied and theoretical electricity, Vol.III, Craiova, iunie 1998.

[7] Ilie F., Bulucea C.A., Popescu M.C., "Simulations of Oil-filled Transformer Loss-of-Life Models", Proceedings of the 11th International Conference on Mathematical Methods and Computational Techniques in Electrical Engineering, Published by WSEAS Press, pp.195-202, Vouliagmeni Beach, Greece, September 2009.

[8] Mastorakis N., Bulucea C.A., Manolea Gh., Popescu M.C., Perescu-Popescu L., "Model for Predictive Control of Temperature in Oil-filled Transformers", Proceedings of the 11th WSEAS International Conference on Automatic Control, Modelling and Simulation, pp.157-165, Istanbul, Turkey, May -June 2009.

[9] Popescu M.C., Degeratu Pr., "Optimal adjustment of the variables of the ambient medium in a room", The 9th symposium on modeling, simulation and identification systems, pp.89-92, Galaţi, Octomber 1996.

[10] Popescu M.C., Manolea Gh., Perescu-Popescu L., Drighiciu A., "Implementation of New Solution Software for Three Tank System Control", Proceedings of the Applied Computing Conference, Published by WSEAS Press, pp.202-208, Vouliagmeni Beach, Greece, September 2009.

[11] Popescu M.C., Valentina E. Balas, Manolea Gh., Perescu L., Mastorakis N., *Theoretical and Practical Aspects of Heating Equation,* WSEAS Transactions on Systems and Control, pp.349-358, Issue 8, Vol.4, August 2009.

[12] Popescu M.C., Olaru O., Mastorakis N., "Processing Data for Colored Noise Using a Dynamic State Estimator", WSEAS Transactions on Communications, Issue 3, Vol.8, pp.321-330, March 2009.

[13] Popescu M.C., Olaru O. and Mastorakis N., *Processing Data for Colored Noise Using a Dynamic State Estimator*, International Journal of Computers and Communications, Issue 3, Vol.2, pp.77-86, 2008.

[14] Popescu, M.C., Balas, M.M., "Thermal Consumptions : Control and Monitoring", 3rd International Workshop on Soft Computing Applications, Library of Congres 2009907136, pp.85-91, Szeged-Hungary-Arad-Romania, July -August 2009.

[15] Popescu M.C., Balas V., Manolea Gh., Mastorakis N., "Regional Null Controllability for Degenerate Heat Equations", Proceedings of the 11th WSEAS International Conference on Sustainability in Science Engineering, pp.32-37,Timisoara, Romania, May 2009.

[16] Popescu M.C., Olaru O, Mastorakis N., "Data Reduction for Signals Observed in Colored Noise", Proceedings of the 10th WSEAS Int. Conf. on Automation & Information, pp.418-424, Prague, March 2009.

[17] Popescu M.C., Petrişor A., Drighiciu M.A., "Modelling and Simulation of a Variable Speed Air-Conditioning System", International Conference on Automation, Quality and Testing, Robotics, Proceedings pp.175-181, Cluj-Napoca, May 2008.

[18] Popescu M.C., Petrisor A., Drighiciu M.A., "Improving Method for Measuring the Elastic & Viscous behaviour of Rubber", Proceedings of the International Conference on Electronics, Computers and Artificial Intelligence, pp.13-19, Number 2/2009, Edited by University of Piteşti, 2009.

[19] Popescu M.C., "Simulation of a temperature control system with distributed parameters", International Conference on Electromechanical and Power Systems, Chişinău, Annals of the University of Craiova, Electrical Engineering, Editura Universitaria, pp.26-32, 2007.

[20] Popescu M.C., Petrişor A., "The experimental Investigation of heat transfer and friction losses interrupted and way fins for fin-and-tube heat exchangers", Buletinul Institutului Politenic din Iaşi, Vol.LII(LVI), pp.1295-1301, 4th International Conferecnce on Electrical And Power Engineering, October 2006.

[21] Popescu M.C., "Thermocuples-Comparative Study", Buletinul Institutului Politenic din Iaşi, Vol.LII(LVI), pp.1069-1074, 4th International Conferecnce on Electrical And Power Engineering, October 2006.

[22] Popescu M.C., "Modelarea şi identificarea fenomenului de recirculare în încăperi cu degajări de nocivităţi", Revista Electrotehnică, Electronică, Automatică, Nr.2/2005, pp.32-40, Editura Electra, Bucureşti, aprilie-iunie 2005.

[23] Popescu M.C., Bulucea C.A, Manolea Gh., Vladu C., "Variables Optimization of Building Air Conditioning System", Proceedings of the 8th WSEAS International Conference on System Science and Simulation in Engineering, pp.226-232, Published by WSEAS Press, Genova, October 2009.

[24] Popescu M.C., "Modelarea fenomenului de recirculare a aerului în cazul unor degajări de căldură", A 40-a Conferinţă Naţională de Instalaţii, secţiunea Instalaţii pentru începutul mileniului trei, Volumul Instalaţii sanitare, încălziri, ventilaţii, gaze, pp.240-245, Editura Matrix Rom, Sinaia, octombrie 2005.